Effects of a bar on optical transmission through Z-shaped metallic slit arrays*

Wu Cai-Ni(吴彩妮)[a], Li Hong-Jian(李宏建)[a)b)†], Peng Xiao(彭 校)[a], Cao Guang-Tao(曹广涛)[b], and Liu Zhi-Min(刘志敏)[a]

[a] College of Physics and Electronics, Central South University, Changsha 410083, China
[b] College of Materials Science and Engineering, Central South University, Changsha 410083, China

(Received 10 August 2012; revised manuscript received 8 November 2012)

We investigate the effects of a bar on optical transmission through Z-shaped metallic slit arrays by using the finite-difference time domain (FDTD) method. A new hybrid Fabry–Perot (FP) surface plasmon polariton (SPP) mode emerges when changing the geometric parameters of the bar, and this mode can be viewed as a coupling between FP mode and SPP mode. In addition, an obvious dip appears in a featured area when the bar deviates from the central line, and a small displacement of the bar leads to tremendous change of the dip. These behaviors can be attributed to the phase resonance. In short, the structure is very sensitive to the metal bar. Furthermore, it combines photonic device miniaturization with sensitivity, which is useful for making optical switches.

Keywords: surface plasmon resonance, transmission, Z-shaped metallic slit arrays

PACS: 73.20.Mf, 78.68.+m, 75.70.−i **DOI:** 10.1088/1674-1056/22/5/057301

1. Introduction

In 1998, Ebbesen *et al.*[1] experimentally demonstrated that an "extraordinary" transmission of light could be obtained through subwavelength hole arrays in metallic films. To date, several physical mechanisms behind the phenomenon of enhanced transmission have been proposed.[2–5] Most researchers believed that the enhanced transmission is attributed to the resonant excitation of surface plasmon (SP) supported by corrugations surrounding the aperture. Moreover, some researchers thought that the resonances of Fabry–Perot (FP) modes in the slit can also give rise to enhanced transmission.[6] The transmission resonance peaks associated with standing wave modes generally appear at $\lambda_N \approx 2nl/N$,[7,8] where λ_N is the wavelength of the N-th order mode, n is the effective refractive index in the slit, and l is the length of the slit. Most importantly, Guillaumee *et al.*[9] found that another type of transmission mode is a hybrid of Fabry–Perot mode and SPP's.[9] In 2004, Lezec and Thio proposed the diffracted wave model which involves the interference of composite evanescent waves generated by diffraction of incident light at the constituent subwavelength surface structure.[10]

Almost all of the parameters have been discussed to adjust the light transmission through slit arrays, such as the period of the slit array,[11,12] interface medium,[13,14] film thickness,[6] and so forth.[15–18] The influence of geometric parameters on the transmission through gold bent slit arrays with Z-shaped channels has also been discussed. It is found that the transmission of the metallic grating with a Z-shaped bent slit array behaves nearly the same as that with a straight slit array with identical slit length.[19] This indicated that the transmission property is promising for reducing the size of photonic devices. However, there exist many difficulties in regulating the parameters of the Z-shaped channel. We need to introduce new parameters to adjust transmission spectrum more easily.

In this work, we introduce a bar to tune the transmission spectrum through gold bent slit arrays with Z-shaped channels by the finite-difference time domain (FDTD) method. Simulation results show that our proposed structure can promise plentiful transmission behaviors by varying the same parameters of the bar as the slit parameters, such as the length and width. In particular, an obvious dip can only emerge in certain areas, and slight movement of the bars leads to tremendous change of the light travel path when the position of the bar varies. Furthermore, the new hybrid FP–SPP mode emerges upon changing the geometric parameters of the bar, and this mode can be viewed as a coupling between FP modes and SPP mode. These new findings are due to the introduction of the bar. Therefore, our research opens a door to a more adjustable and multifunctional metal grating.

2. Metallic structures and simulation method

Figure 1 depicts schematically a unit cell of the Z-shaped metallic grating. The period and thickness of the grating are $p = 750$ nm and $h = 500$ nm, respectively. A grating slit, with width w and length s_1, s_2, or s_3 is modified by a transversely located bar parallel to the left part of the Z-shaped

*Project supported by the Specialized Research Fund for the Doctoral Program of Higher Education of China (Grant No. 20100162110068) and the National Natural Science Foundations of China (Grant Nos. 61275174 and 11164007).

†Corresponding author. E-mail: lihj398@yahoo.com.cn

© 2013 Chinese Physical Society and IOP Publishing Ltd

slit. The central length of the Z-shaped slit is defined as $l = s_1 + s_2 + s_3 - 2w$. As shown in Fig. 1, the size and location of the bar in this work are adjusted to disturb the grating slightly. Hence, the width w' and length s' of the bar, as well as the distance from the central line d, are changed in a certain range.

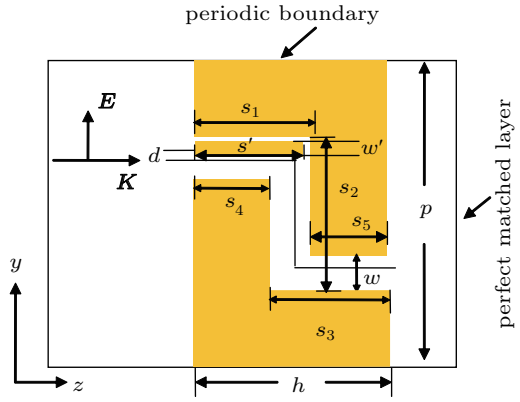


Fig. 1. (color online) Scheme of a unit cell of the period metallic grating.

In our two-dimensional (2D) FDTD calculations,[20,21] we simulate the structure with a computational window of $L_y \times L_z = 750\ \text{nm} \times 5250\ \text{nm}$, where the structure in the x direction is uniform and infinite. Periodic boundary conditions are used above and below the slits along the y direction, while perfectly matched layers (PMLs)[22] are applied on both the left and right surfaces of the computational space, which results in a distance of 2250 nm from the interface of the gold film along the z direction. The detecting location is set to be 287.5 nm from the rear surface of the gold film, and the transmission is normalized without a metallic structure. The spatial mesh cells are set to be $\Delta y = \Delta z = 3.5$ nm, and the time step is taken to be $\Delta t = \Delta y/2c$ (c is the light velocity in a vacuum). The prepared structure is excited by an ultrashort linearly-polarized pulse. The incident light is considered to polarize along the y axis and irradiate the structure along the z direction in our work. Here, the metal is chosen to be gold (Au). The frequency-dependent permittivity of the metal is described by the Drude model as

$$\varepsilon(\omega) = 1 - \omega_p^2/(\omega^2 + i\omega\gamma_p), \tag{1}$$

where the plasma frequency $\omega_p = 1.37 \times 10^{16}$ Hz, the damping rate $\gamma_p = 4.08 \times 10^{13}$ Hz,[23] and ω is the angle frequency of the incident wave.

3. Results and discussion

First of all, figure 2(d) depicts the calculated transmission spectra of Z-shaped slit arrays with different values of width w' of the bar with the length $s' = 262.5$ nm and the distance $d = 0$ nm. As shown in Fig. 2(d), there are two transmission peaks in each of the transmission spectra of the bar bent slit array. Based on Ref. [19], the shorter-wavelength transmission resonance peak is mostly associated with the surface plasmon resonance, while the longer-wavelength peak is relevant to the localized waveguide resonance for the periodic metal slit array with Z-shaped channels. The localized waveguide resonance mode is characterized by constructive interference along the channel between all partial transmitted waves, in the way of FP cavity mode.[24] By introducing the bar, we can see that a higher-order mode in the shorter wavelength region appears as the bar width increases. Particularly, this new mode is red-shifted and decreases with the other two resonance modes. The longer-wavelength resonance peak is red-shifted obviously. Figures 2(a)–2(c) show electric field distributions corresponding to three peaks at wavelengths of 812.9, 1082, and 1856 nm, respectively, with the bar width w' being 50 nm. Based on Ref. [9], there is a continuous change from FP-related peaks to SPP-related peaks, and the transmission modes are a hybrid of FP mode and SPP mode. The coupling between the SPP mode and FP mode is apparently enhanced, which is attributed to the constructive interference. As shown in Figs. 2(a)–2(c), the intensity of electric field E_z at $\lambda = 1082$ nm is stronger than that at $\lambda = 812.9$ nm and 1856 nm. We consider that the second peak is in the FP–SPP mode, which results from the coupling between the SPP mode and FP mode. Thus, the transmission peaks can be grouped into three types: (i) surface resonance peak at $\lambda = 812.9$ nm (judging from period p of this structure, it is 750 nm), (ii) FP mode at $\lambda = 1856$ nm, and (iii) hybrid FP–SPP mode at $\lambda = 1082$ nm.

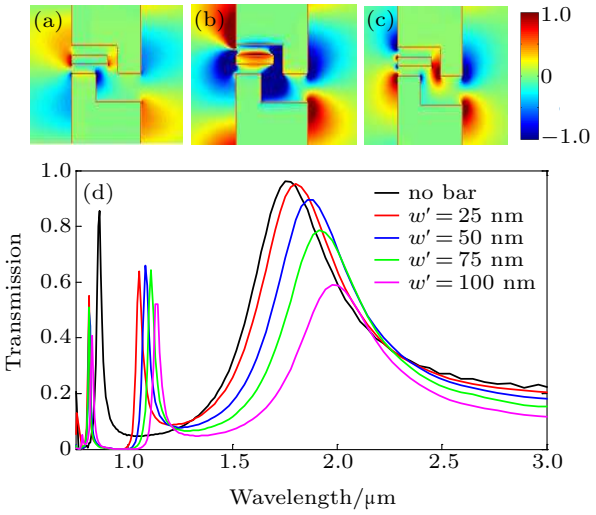


Fig. 2. (color online) Values of electric field E_z at (a) $\lambda = 812.9$, (b) 1082, and (c) 1856 nm for width $w' = 50$ nm. (d) Transmission spectra through metallic grating with film thickness $h = 500$ nm, central slit length $l = 650$ nm, and length $s' = 262.5$ nm for different widths of the bar.

The transmission behavior of the FP mode can be explained by the proposed model in Ref. [25]. It is universally received that the resonance in a slit array with perpendicular

cuts is attributed to three factors: the FP cavity, the surface current flow, and the surface charge.[26] Even though the structure considered here is different from that in Ref. [25], both structures have similar mechanisms. The bare metallic slit can be treated as an FP cavity. The resonant wavelength of FP mode in a bare slit array can be expressed by

$$2kL_{\mathrm{FP}} + \theta = 2N\pi, \tag{2}$$

where $k = 2n\pi/\lambda$ is the wave number, L_{FP} is the length of the cavity, θ is the total phase reflected at the ends of the slits, and N is the correlation integer. For the smooth slit, current density standing waves are established with opposite signs on both metal walls of each slit by oscillating incident light. The slit can be considered as a parallel-plate capacitor and the capacitance is used to describe the ability to accumulate charges. Introducing the bar is equivalent to shortening the length of current flow. The decrement in the effective FP cavity can be expressed as δ_{J}. Besides surface current flow standing waves, surface charge standing waves are also established on the walls of the slit. The appearance of the bar is equivalent to the increase in the length of the slit, the increment is denoted by δ_{Q}. The total effect of the bar on the effective length of the FP cavity is determined by $L_{\mathrm{eff}} = L_{\mathrm{FP}} + \delta_{\mathrm{Q}} - \delta_{\mathrm{J}}$. If $\delta_{\mathrm{Q}} > \delta_{\mathrm{J}}$, the effective length is larger than the actual length, the resonant wavelength becomes larger. If $\delta_{\mathrm{Q}} < \delta_{\mathrm{J}}$, the resonant wavelength becomes smaller. The charge densities and surface currents on the slit walls can be obtained from $\boldsymbol{n} \times \boldsymbol{H} = \boldsymbol{J}$ and $\boldsymbol{n} \cdot \boldsymbol{D} = \sigma$, respectively, where $\boldsymbol{n}$ is the unit normal vector directed from metal into air in slit, $\boldsymbol{H}$ and $\boldsymbol{D}$ are the magnetic field and electric displacement, and $\boldsymbol{J}$ and σ are the surface current density and charge density, respectively. When the bar is located in the center of the antinodes (nodes) of the electric (magnetic) field, the bar has the strongest influence on the charge density but a weak effect on the current density, so that $\delta_{\mathrm{Q}} > \delta_{\mathrm{J}}$ and the effective length of the FP cavity increases. As a consequence, corresponding wavelength of the resonance peak becomes larger for the same order FP mode based on Eq. (2), and the FP mode is red-shifted. In addition, the reduction of the FP mode is associated with the energy loss inside the slit.

Compared with the FP mode, the surface plasmon resonance mode is red-shifted slightly. The wavelength that corresponds to an in-plane surface plasmon resonance can be expressed as[27]

$$\lambda = \frac{p}{\sqrt{i^2 + j^2}} \sqrt{\frac{\varepsilon_{\mathrm{d}} \varepsilon_{\mathrm{m}}}{\varepsilon_{\mathrm{d}} + \varepsilon_{\mathrm{m}}}}, \tag{3}$$

where p is the grating period, i and j are integers, ε_{d} and ε_{m} are the relative dielectric constants of metal and dielectric, respectively, and $\sqrt{\varepsilon_{\mathrm{d}} \varepsilon_{\mathrm{m}}/(\varepsilon_{\mathrm{d}} + \varepsilon_{\mathrm{m}})}$ is the effective refractive index. Effective refractive index of the structure increases with bar width increasing, so λ becomes larger, which means that the surface plasmon resonance mode is red-shifted, and the decrease of the surface plasmon resonance transmission magnitude is attributed to the weak lateral coupling between slits as the bar width increases.

Based on Ref. [28], far from the crossing point, the modes have either a well defined FP-mode or surface-mode character. Conversely, close to the crossing point, the modes are in the strong coupling regime and cannot be called either surface modes or FP modes. Hence, the concept of coupled mode is introduced. This concept allows the reconciliation of the different points of view given in the literature to explain this phenomenon. As shown in Fig. 2(d), the coupled mode is red-shifted, and its value decreases accompanied by the other two modes. The FP–SPP mode is a hybrid of FP mode and SPP mode. As a consequence, its nature is influenced by FP mode and SPP mode. Both the FP mode and SPP mode are red-shifted and apparently decrease, which resembles the scenario of the coupled mode.

Figure 3 shows the transmission spectra for Au metallic slit arrays with Z-shaped channels with different bar lengths, bar width $w' = 50$ nm , slit length $l = 650$ nm, slit width w= 150 nm, and film thickness h= 500 nm. It is found that the FP mode red-shifts compared with the transmission spectrum of the Z-shaped metallic bent slit and then it keeps the same wavelength 1856 nm until the bar length increases to 325 nm ($s' = s_1$). By changing the length s', a new coupled mode appears and red-shift takes place with the increase in length. As shown in Fig. 3, the surface plasmon resonance mode is blue-shifted when the bar length $s' > 175$ nm and its value first decreases and then increases.

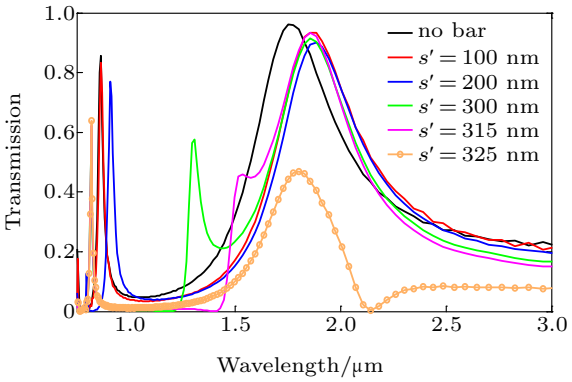


Fig. 3. (color online) Transmission spectra through metallic grating with film thickness $h = 650$ nm, central slit length $l = 650$ nm, and bar width $w' = 50$ nm for different lengths of the bar.

As stated above, the FP mode is red-shifted due to the introduction of the bar, then kept at 1856 nm until the length of the bar reaches 325 nm. This is because the FP mode is influenced by the FP cavity. The introduction of the bar changes the shape of the cavity, which causes the red-shift of the FP mode. By changing the length, the FP cavity varies slightly and the FP mode is kept at 1856 nm. However, when the length s'

is equal to s_1, the FP resonance mode decreases and is blue-shifted because all light from the above cavity is prevented by the bar.

The bar divides the left top section of the Z-shaped waveguide into two parts and propagation behaviors of the surface plasmon in these two parts are alike when the length s' is not larger than 175 nm ($s_4 = 175$ nm). As a result, the surface plasmon resonance peak is kept at 963.7 nm. Once $s' >$ 175 nm, the surface plasmon resonance peak is blue-shifted, while both a forbidden band and an FP–SPP coupled mode appear. As the coupled mode is red-shifted, the forbidden band width increases accordingly. Finally, the mode is gradually combined with the FP mode when the bar length approaches 325 nm. These transmission behaviors can be explained by the variation of coupling between FP mode and SPP mode under the condition of $s' > 175$ nm. The top and bottom cavities are different when $s' > 175$ nm, which leads to the variation of coupling.

In Fig. 4(a), we fix the bar length $s' = 262.5$ nm and the width $w' = 50$ nm and vary the distance d from 0 to 50 nm. The FP resonance peak splits into two peaks in the transmission spectrum when distance d achieves 45 nm, and an obvious transmission dip emerges. From Fig. 4(a), we can find that the separation between FP resonance modes, the coupled mode, and the surface resonance mode can be tuned by shifting the position of the bar. The coupling between FP mode and SPP mode gives rise to the coupled mode, and regulating the position of the bar can lead to a red-shift of the coupled mode.

The physical origin of the transmission dip can be explained in terms of phase resonance as follows.[29,30] On the one hand, it is well known that for a single periodic hole array, the translation invariance can reduce the field degrees of freedom to just a unit cell. Therefore, the fields in all holes are equal when a plane wave is normally incident. As for compound periodic hole arrays, this translation invariance can also reduce the degrees of freedom to a unit cell, but it cannot ensure that the fields of different holes in a unit cell are identical. On the other hand, the FP resonance arises from individual hole slits, so the addition of extra hole slits to each unit cell can introduce new FP modes (new degrees of freedom). The FP modes induced by different holes in a unit cell are degenerate if the holes have identical area, or non-degenerate if these hole areas are different. For the non-degenerate case, it is understandable that the field phases in different holes are unequal.[29,30] As for the structure displaced in this work, if the bar is located at the central line of the slit ($d = 0$ nm), the two sections separated by the bar are equal. It is equivalent to a single periodic slit array, and the field phases in the two sections are equal due to the symmetry. If the bar lies at different positions, it affects the current density and charge density in a different way due to the asymmetry, which provides new degrees of freedom for the field phase distribution. When the phase difference between the two sections approaches π, an obvious dip resulting from destructive interference between these two slits is present in the transmission spectrum.

In order to understand the dependence of phase resonance on the position of the bar well, we proceed with more subtle distance variation from $d = 40$ to 50 nm with a step of 2.5 nm (see Fig. 4(b)). It is found that an obvious dip appears in a featured area from $d = 45$ to 49 nm, which leads to the splitting of FP resonance peak. Furthermore, a new coupled mode with a small value occurs near the surface resonance mode in this area, which cannot be observed in an area of 0–45 nm. Therefore, the slight movement of the bar causes tremendous change of FP resonance mode. At this point, the structure can be used in an optical switch. Moreover, there is a zero transmission wave all the time in the featured area, and this result may be useful for making adjustable filters.

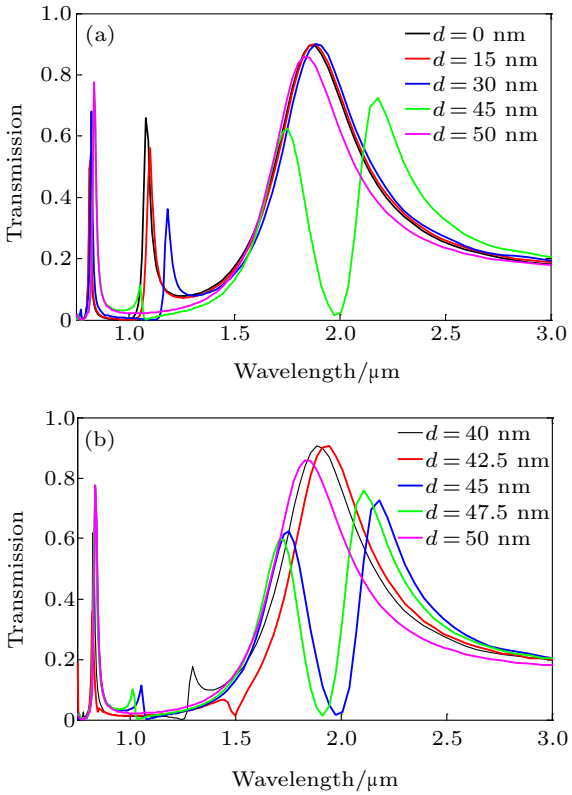


Fig. 4. (color online) (a) Transmission spectra for different positions of the bar with $s' = 262.5$ nm and $w' = 50$ nm. (b) Transmission spectra for subtle variation of the distance d with $s' = 262.5$ nm and $w' = 50$ nm.

Under the condition of the bar length $s' = 262.5$ nm, width $w' = 50$ nm, and $d = 45$ nm, the transmission spectra are shown in Fig. 5(d). It is found that the maximal (minimum) transmission always accompany the minimum (maximal) reflection. Figures 5(a)–5(c) show the contour profiles of field H_x for two FP resonance peaks and the transmission dip at $\lambda = 1752$, 1974, and 2181 nm, respectively. From these profiles, the filtering effect is clearly observed. The center wavelength of the transmission dip is 1974 nm that is the same as

that of the reflection peak. The coupling between resonators is strongly confined by destructive interference, and promoted by constructive interference. The cooperative coupling effect induces the electromagnetic energy to be coupled back in the Z-shaped waveguide, destructive interference, and a suppressed state in the cavity with much weaker magnetic field. This suggests that the lost energy is reflected back to the left side. It can also be shown from Fig. 5(b) that intense magnetic fields exist on the left side of the incident plane for $\lambda = 1974$ nm, which indicates large reflection.[31] Figures 5(a) and 5(c) show the values of magnetic field H_x at 1752 and 2181 nm, respectively, which correspond to the central wavelengths of the two peaks that result from the splitting of the FP resonance peak. However, in Fig. 5(a), the effects of the bar on the magnetic field are contrary to those in Fig. 5(c), which indicates that the main reason for the occurrence of the transmission dip is related to the circumstance that the two slits resonate out of phase with each other at the intermediate frequency of $\lambda = 1974$ nm. It is the destructive interference between the electromagnetic fields in the two slits that destroys the interference pathway forming the transmission peak and allows the incident light to propagate through the structure uninhibited.

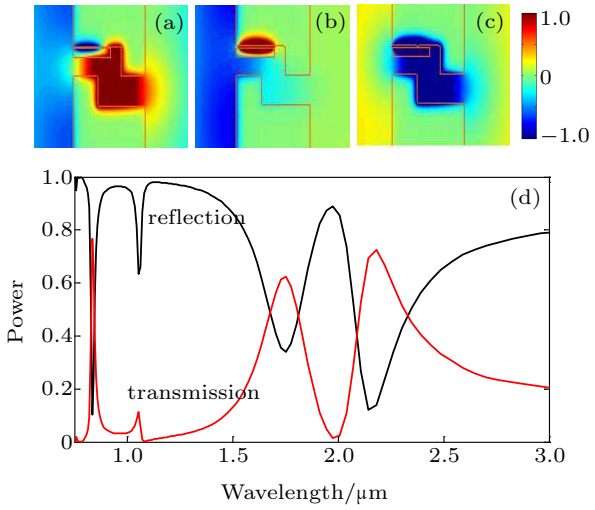


Fig. 5. (color online) Values of magnetic field H_x at wavelength of (a)1752 nm, (b) 1974 nm, and (c) 2181 nm. (d) Transmission and reflection spectra when the bar length $s' = 262.5$ nm, width $w' = 50$ nm, and separation between central lines $d = 45$ nm.

In the proposed structure, we introduce a transversely located gold strip as a bar for tuning the effective refractive index and controlling the phase change. Thus, the structure prepared in this work can have a promising application to optical switch by SPP excitation, which is tunable and has strong modulation ability and compact footprint. Some relevant studies have reported applications of the proposed structure by the modern technology. Srituravanich *et al.*[32] reported on a technology of flying plasmonic lens in the near field for high-speed nanolithography and nanoscale metrology and imaging. Hence, the position of the bar can be moved and the transmission of the Z-shaped metallic slit array can be controlled accurately. Above all, the proposed structure can be fabricated and could find important applications for highly integrated optical circuits.

4. Conclusion

In this paper, we investigate the transmission properties of a Z-shaped metallic slit array with a transversely located gold bar by using 2D FDTD method. It is found that the surface resonance peak and FP resonance peak are adjusted easily by the bar. All peaks are red-shifted and decrease with the increase of the width of the bar. These behaviors can be explained by the FP cavity theory. In addition, the variation of the bar length causes the coupled mode to be red-shifted while the FP resonance peak remains unchanged. The results confirm the FP–SPP mode theory. Most importantly, an obvious dip emerges when the bar deviates from the central line and gradually approaches the top slit edge. This transmission behavior results from the phase resonance arising from the coupling between these two new slits, which are characterized by the π phase difference between adjacent slits and indicated by a sharp dip in the transmission spectrum. The slight variation of the bar leads to a tremendous change of transmission, which provides a promising application in optical switches and filters.

References

[1] Ebbesen T W, Lezec H J, Ghaemi H F, Thio T and Wolff P A 1998 *Nature* **391** 667
[2] Cao Q and Lalanne P 2002 *Phys. Rev. Lett.* **88** 057403
[3] Gay G, Alloschery O, Viaris de Lesegno B, Weiner J and Lezec H J 2006 *Phys. Rev. Lett.* **96** 213901
[4] Medina F, Ruiz-Cruz J A, Mesa F, Rebollar J M, Montejo-Garai J R and Marqués R 2009 *Appl. Phys. Lett.* **95** 071102
[5] Wang J F, Li H J, Zhou Z Y, Li X Y, Liu J and Yang H Y 2010 *Chin. Phys. B* **19** 117310
[6] Jiao X, Wang P, Tang L, Lu Y, Li Q, Zhang D, Yao P, Ming H and Xie J 2005 *Appl. Phys. B* **80** 301
[7] Takakura Y 2001 *Phys. Rev. Lett.* **86** 5601
[8] Hibbins A P, Lockyear M J and Sambles J R 2006 *J. Appl. Phys.* **99** 124903
[9] Guillaumee M, Andrea Dunbar L and Satanley R P 2011 *Opt. Express* **19** 4740
[10] Lezec H J and Thio T 2004 *Opt. Express* **12** 3629
[11] Porto J A, García-Vidal F G and Pendry J B 1999 *Phys. Rev. Lett.* **83** 2845
[12] Sun M, Tian J, Li Z Y, Cheng B Y, Zhang D Z, Jin A Z and Yang H F 2006 *Chin. Phys. Lett.* **23** 486
[13] Kihm J E, YoonY C, Park D J, Ahn Y H, Ropers C, Lienau C, Kim J, Park Q H and Kim D S 2007 *Phys. Rev. B* **75** 035414
[14] Wang X D, Ye L H, Ma J and Jiang M P 2010 *Chin. Phys. Lett.* **27** 094101
[15] Gordon R 2007 *Phys. Rev. B* **75** 193401
[16] Fu S L, Li H J, Xie S X, Zhou X, Xu H Q and Xia H 2011 *Chin. Phys. B* **20** 087302
[17] Yu X Q, Zhou L, Zhu Y Y and Zhu S L 2008 *Chin. Phys. Lett.* **25** 274
[18] Hu B, Gu B Y, Dong B Z and Zhang Y 2008 *Appl. Phys. Lett.* **92** 151901
[19] Xie S X, Li H J, Zhou X, Xu H Q and Liu Z M 2011 *J. Opt. Soc. Am. A* **28** 441

[20] Taflove A and Hagness S C 2005 *Computational Electrodynamics: the Finite-Difference Time-Domain Method* (2nd edn.) (Boston: Artech House)

[21] Yee K S 1966 *IEEE Trans. Antennas Propag.* **14** 302

[22] Berenger J P 1994 *J. Comput. Phys.* **114** 185

[23] Ordal M A, Long L L, Bell R J, Bell S E, Bell R R, Alexander R W and Ward C A 1983 *Appl. Opt.* **22** 1099

[24] Hibbins A P, Lockyear M J and Sambles J R 2005 *Appl. Phys. Lett.* **87** 263116

[25] Wang Y, Wang Y, Zhang Y and Liu S 2009 *Opt. Express* **17** 5014

[26] He M D, Gong Z Q, Li S, Luo Y F, Liu J Q and Chen X S 2010 *Solid State Commun.* **150** 1283

[27] Kihm J E, Yoon Y C, Park D J, Ahn Y H, Ropers C, Lienau C, Kim J, Park Q H and Kim D S 2007 *Phys. Rev. B* **75** 035414

[28] Marquier F, Greffet J J, Collin S, Pardo F and Pelouard J L 2005 *Opt. Express* **13** 70

[29] Liu Z F and Jin G J 2009 *J. Phys: Condens. Matter* **21** 445401

[30] Liu Z M, Li H J and Xie S X 2011 *Opt. Express* **19** 4217

[31] Han Z H and Bozhevolnyi S I 2011 *Opt. Express* **19** 3251

[32] Srituravanich W, Pan L, Wang Y, Sun C, Bogy D B and Zhang X 2008 *Nature Nanotechnol.* **3** 733